Korea-Australia Rheology Journal
Vol. 18, No. 4, December 2006 pp. 199-207

Nonlinear rheology of polymer melts: a new perspective on finite chain extensibility effects

Manfred H. Wagner*
TU Berlin, Polymertechnik/Polymerphysik, Fasanenstrasse 90, D-10623 Berlin, Germany
(Received November 5, 2006)

Abstract

Measurements by Luap *et al.* (2005) of elongational viscosity and birefringence of two nearly monodisperse polystyrene melts with molar masses M_W of 206,000 g·mol^{-1} (PS206k) and 465,000 g·mol^{-1} (PS465k) respectively are reconsidered. At higher elongational stresses, the samples showed clearly deviations from the stress optical rule (SOR). The elongational viscosity data of both melts can be modeled quantitatively by the MSF model of Wagner *et al.* (2005), which is based on the assumption of a strain-dependent tube diameter and the interchain pressure term of Marrucci and Ianniruberto (2004). The only nonlinear parameter of the model, the tube diameter relaxation time, scales with M_W^2. In order to get agreement with the birefringence data, finite chain extensibility effects are taken into account by use of the Padé approximation of the inverse Langevin function, and the interchain pressure term is modified accordingly. Due to a self-regulating limitation of chain stretch by the FENE interchain pressure term, the transient elongational viscosity shows a small dependence on finite extensibility only, while the predicted steady-state elongational viscosity is not affected by non-Gaussian effects in agreement with experimental evidence. However, deviations from the SOR are described quantitatively by the MSF model by taking into account finite chain extensibility, and within the experimental window investigated, deviations from the SOR are predicted to be strain rate, temperature, and molar mass independent for the two nearly monodisperse polystyrene melts in good agreement with experimental data.

1. Stress optical rule

The well established stress optical rule (SOR) can be expressed as $\underline{\underline{\Delta n}} = C\underline{\underline{\sigma}}$, where $\underline{\underline{\Delta n}}$ is the anisotropic part of the refractive index tensor, $\underline{\underline{\sigma}}$ represent the extra stress tensor and C is the so called stress optical coefficient (SOC), the latter being largely independent of molar mass, molar mass distribution, polymer concentration, shear rate and temperature (Lodge, 1955; Philippoff, 1956), but dependent on the monomer chemistry (Janeschitz-Kriegl, 1983). Essentially, the SOR states that the mechanical and optical tensors are coaxial and proportional to each other.

The validity of the SOR for homogeneous, isotropic polymer melts under a wide range of deformation conditions was confirmed by Wales (1976) and Janeschitz-Kriegl (1983). Furthermore, the SOR is crucial because it bridges the macroscopic stress with the microscopic processes, i.e. the rotations and deformations of the atomic bonds (Wales, 1976), and its validity for polymer melts is an indication of the validity of Gaussian chain statistics. Recently, the importance of this rule was even shown in the injection-compression molding of optical media like compact discs or digital video discs (Fan *et al.*, 2004).

Violations of the SOR under certain conditions were reported either for polymer melts (Matsumoto and Bogue, 1977; Muller and Froelich, 1985; Kotaka *et al.*, 1997), solutions (Cathey and Fuller, 1990; Talbott and Goddard, 1979; Pellens *et al.*, 2005) or networks (Subramanian and Galiatsatos, 1993). Different origins of the failure of the SOR were discussed, e.g. the influence of the molecular weight distribution (van Meerveld, 2004), the chain conformation (Sridhar *et al.*, 2000), or the role of the number of entanglements in the fluid (Rothstein and McKinley, 2002). Certain types of systems do not follow the SOR at all like rod-like polymers (Mead and Larson, 1990). Additionally, experimental conditions can lead to the failure of the SOR, like performing experiments near the glass transition temperature (Wales, 1976; Inoue *et al.*, 1991; Muller and Pesce, 1994; Kröger *et al.*, 1997), where energetic contributions to the stress may become important.

Failure of the SOR is expected under "fast flow" conditions, e.g. in an elongational experiment at a rate higher than the inverse of the Rouse time of the chain, which would impose such a high stretching regime on the polymer chains (Venerus *et al.*, 1999) that they would no longer

*Corresponding author: Manfred.Wagner@TU-Berlin.DE

obey Gaussian chain statistics (Mead and Leal, 1995). In this case, which is the subject of the present work, the SOR fails, because while birefringence saturates, the stress continues to grow unboundedly.

2. Nonlinear rheology of polymer melts

The original Doi-Edwards (DE) model relates the macroscopic stress to chain orientation only, assuming the tension in the chain segments to be at their equilibrium value after a fast retraction process, which takes place within a Rouse time τ_R (Doi and Edwards, 1978; Doi and Edwards, 1979), thereby ignoring the possibility of chain stretching. As a consequence, the nonlinear behavior in general extensional flows is not well predicted by the DE model (Wagner, 1990; Wagner *et al.*, 2005). Another shortcoming of ignoring chain stretch is the prediction of a steady-state elongational viscosity η_{ss} scaling with the strain rate $\dot{\varepsilon}$ as $\eta_{ss} \propto \dot{\varepsilon}^{-1}$ (Doi and Edwards, 1979). To avoid the DE model limitations, theories accounting for chain stretch have been proposed (e.g. Marrucci and Grizzuti, 1988; Pearson *et al.*, 1991; Mead and Leal, 1995; Mead *et al.*, 1998; Hua and Schieber, 1998; Öttinger, 1999; Fang *et al.*, 2000) with the general idea that chain stretching starts to be significant at Deborah numbers $De = \dot{\varepsilon}\tau_R > 1$. However, as Fig. 1 demonstrates, this assumption is not in agreement with experimental evidence for monodisperse polystyrene melts (Wagner *et al.*, 2005). Even when introducing finite chain extensibility effects (FENE) into these models, the scaling of the steady-state elongational viscosity η_{ss} with the strain rate $\dot{\varepsilon}$ is predicted incorrectly, as demonstrated in Fig. 2.

On the other hand, extensional measurements of nearly monodisperse polystyrene melts have shown a power-law dependence of the steady-state elongational viscosity, which deviates significantly from the DE prediction, and

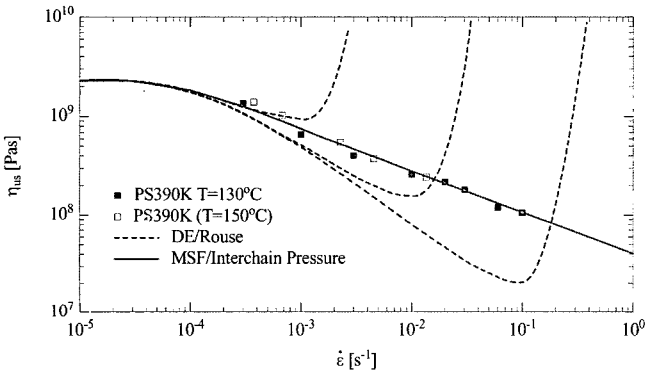

Fig. 1. Comparison of measured steady-state elongational viscosity data of PS390 K (symbols) to predictions by MSF model with chain stretch balanced by linear spring force (dotted lines, from left to right: τ_R=329s/32.9s/3.29s) and by interchain pressure (full line, τ_a=1462s).

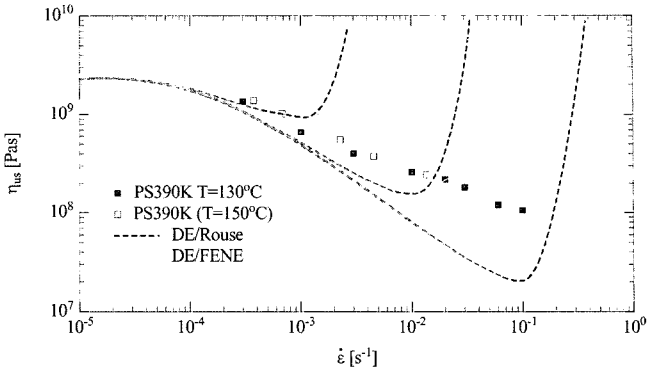

Fig. 2. Comparison of measured steady-state elongational viscosity data of PS390K (symbols) to predictions by MSF model with chain stretch balanced by linear spring force (dotted lines) and FENE spring force (full lines). From left to right: τ_R=329s/32.9s/3.29s.

scales approximately as $\eta_{ss} \propto \dot{\varepsilon}^{-1/2}$ (Bach *et al.*, 2003). To explain this behavior, Marrucci and Ianniruberto (2004) modified the DE model by allowing for tube contraction due to the applied deformation, which is balanced by an internal chain pressure against the tube wall. By use of scaling arguments, they derived indeed qualitatively the observed scaling of the steady-state elongational viscosity.

Based on the Molecular Stress Function (MSF) model (Wagner *et al.*, 2001) and assuming a balance between affine chain deformation and the interchain pressure term of Marrucci and Ianniruberto, not only the steady-state, but also the transient elongational viscosities of 4 nearly monodisperse polystyrene melts could be modeled quantitatively (Wagner *et al.*, 2005) by use of a single non-linear material parameter, the tube diameter relaxation time τ_a. It is worth mentioning that for the highest molar mass polystyrene PS390K, a scaling of the steady-state elongational viscosity close to $\eta_{ss} \propto \dot{\varepsilon}^{-0.4}$ was predicted, which is not only in qualitative but in quantitative agreement with experimental evidence (see Fig. 1).

At higher elongation rates, considerable relative stretch of macromolecular chains is predicted (Fig. 3), which raises the question of the validity of Gaussian chain statistics.

Luap and coworkers (2005) performed simultaneous stress and birefringence measurements during elongation of two similar polystyrene melts with narrow molar mass distribution. They confirmed the experimental results of Bach *et al.* (2003) of an increasing strain hardening effect and a continuous decrease of the steady-state elongational viscosity with increasing strain rate. Furthermore, they found that the SOR was no longer valid at higher strain rates due to the amount of chain stretching achieved, which indicates that the chains are deformed outside the validity of Gaussian chain statistics.

In this contribution, we reconsider the Molecular Stress

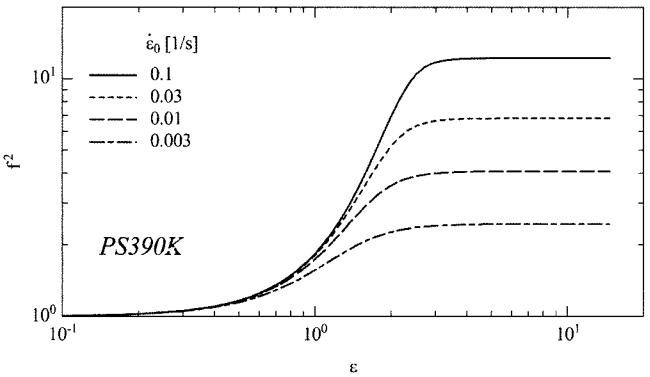

Fig. 3. Square of relative stretch of macromolecular chains of PS390 K as predicted by MSF model with τ_a=1462s for different elongation rates.

Function model based on the interchain pressure concept of Marrucci and Ianniruberto (2004) by taking into account non-Gaussian chain extensibility in the interchain pressure term. The aim is to model simultaneously and quantitatively not only the transient and steady-state elongational viscosities of the two polystyrene melts studied by Luap *et al.* (2005), but also the experimentally observed deviations from the SOR.

3. Experimental data

The experimental data discussed are those of Luap *et al.* (2005). Elongational experiments at constant strain rate were performed to determine at the same time tensile stress and flow-induced birefringence. Two polystyrenes with mass-average molar masses of 206,000 g·mol^{-1} (PS206k) and 465,000 g·mol^{-1} (PS465k), and polydispersities of 1.04 and 1.08 respectively were investigated. The experiments were performed at 140°C and 150°C for the PS206k, and at 150°C and 160°C for the PS465k. Standard time-temperature shifting according to the WLF equation with c_1=6.8 and c_2=98 K for T_0=150°C was used. We derived discrete relaxation spectra with partial moduli g_i and relaxation times λ_i by use of the IRIS program (Winter and Mours, 2003) from the linear-viscoelastic master curves of G' and G'' at a reference temperature of 150°C. Molecular characterization and relaxation spectra are summarized in Table 1.

4. Molecular stress function (MSF) model with finite extensibility

The MSF model (Wagner and Schaeffer, 1992; Wagner *et al.*, 2001; 2003) is a single tube segment model, which allows predicting quantitatively the rheology of polymer melts in extension and shear. In this theory, the tube diameter a is assumed to be independent of the orientation of tube segments, and to decreases from its equilibrium value a_0 to a value a with increasing deformation.

Table 1. Molecular characterization and relaxation spectra of PS samples at 150°C

PS206k		PS465k	
Mw=206,000 *g/mol*		Mw=465,000 *g/mol*	
PD=1.04		PD=1.08	
$J_e^0=1.29x10^{-5}$ [Pa^{-1}]		$J_e^0=1.84x10^{-5}$ [Pa^{-1}]	
$\eta_0=2.35x10^6$ [$Pa\cdot s$]		$\eta_0=2.66x10^7$ [$Pa\cdot s$]	
τ_a=14*s*		τ_a=71*s*	
τ_R=2.4*s*		τ_R=9.6*s*	
g_i [Pa]	λ_i [s]	g_i [Pa]	λ_i [s]
3.186×10^5	2.93×10^{-3}	1.421×10^6	4.685×10^{-4}
4.582×10^6	1.336×10^{-4}	1.343×10^5	1.436×10^{-2}
8.121×10^4	3.491×10^{-2}	3.856×10^4	2.78×10^{-1}
4.786×10^4	345×10^{-1}	4.644×10^7	4.36×10^{-6}
5.498×10^4	2.45	4.305×10^4	3.062
6.716×10^4	1.638×10^1	5.782×10^4	2.743×10^1
2.274×10^4	4.826×10^1	7.782×10^4	2.287×10^2
		5.592×10^3	1.262×10^3

The extra stress tensor $\underline{\underline{\sigma}}(t)$ of the MSF model is given by a history integral of the form

$$\underline{\underline{\sigma}}(t)=\int_{-\infty}^{t} m(t-t')f\lambda\underline{\underline{S}}_{DE}^{IA}(t,t')dt' \tag{1}$$

The strain measure $\underline{\underline{S}}_{DE}^{IA}$ represents the contribution to the extra stress tensor originating from the affine rotation of the tube segments assuming "Independent Alignment (IA)" (Doi and Edwards, 1978), and is given by

$$\underline{\underline{S}}_{DE}^{IA}(t,t')\equiv 5\left\langle\frac{\underline{u}'\underline{u}'}{u'^2}\right\rangle_0=5\underline{\underline{S}}(t,t') \tag{2}$$

with $\underline{\underline{S}}=\underline{\underline{S}}(t,t')$ being the relative second order orientation tensor. $\underline{u}'\underline{u}'$ is the dyad of a deformed unit vector $\underline{u}'=\underline{u}'(t,t')$,

$$\underline{u}'=\underline{\underline{F}}_t^{-1}\cdot\underline{u} \tag{3}$$

$\underline{\underline{F}}_t^{-1}=\underline{\underline{F}}_t^{-1}(t,t')$ is the relative deformation gradient tensor, and u' is the length of $\underline{u}'$. The orientation average is indicated by $\langle\ldots\rangle_0$,

$$\langle\ldots\rangle_0\equiv\frac{1}{4\pi}\oint[\ldots]\sin\theta_0 d\theta_0 d\varphi_0 \tag{4}$$

i.e. an average over an isotropic distribution of unit vectors $\underline{u}$.

To account for finite chain extensibility effects, stretch λ and relative tension f (in the following called "molecular stress") of a chain have to be distinguished. $\lambda=\lambda(t,t')$ rep-

resents the inverse of the relative tube diameter a/a_0, and at the same time the relative length of a deformed tube segment,

$$\lambda(t,t') = \frac{a_0}{a(t,t')} = \frac{l(t,t')}{l_0} \tag{5}$$

t' indicates the time when the tube segment was created with equilibrium tube diameter a_0 and equilibrium length l_0.

In the Gaussian limit, the molecular stress function f is equal to the tube stretch λ. However, this is valid only as long as $\lambda<0.5\,\lambda_m$ (Bird *et al.*, 1987), where $\lambda_m \cong \sqrt{n}$ represents the maximum stretch (i.e. a fully extended chain), and n the number of Kuhn steps in a tube segment. Outside the Gaussian regime, tension in the chain can be described by the inverse Langevin function, or, due to its mathematical complexity, approximations of it, like the so- called Warner (Larson, 1988) or Padé approximations (Cohen, 1991). Since the latter version seems to be more accurate, nonlinear elasticity caused by finite extensibility (FENE) is implemented in the MSF theory in the following way:

$$f = c(\lambda)\lambda \tag{6}$$

c is a nonlinear spring coefficient, representing a relative Padé inverse Langevin function with (Ye and Sridhar, 2005)

$$c(\lambda) = \frac{\left(3-\frac{\lambda^2}{\lambda_m^2}\right)\cdot\left(1-\frac{1}{\lambda_m^2}\right)}{\left(3-\frac{1}{\lambda_m^2}\right)\cdot\left(1-\frac{\lambda^2}{\lambda_m^2}\right)} \tag{7}$$

While $\underline{\underline{S}}_{DE}^{IA}$ is determined directly by the deformation history according to Eq. (3), λ is found as solution of an evolution equation taking into account affine tube segment deformation balanced by the interchain pressure. From the DE theory, Marrucci and Ianniruberto (2004) derived an interchain pressure term of the form $p \propto \frac{a_0^2 V_0}{a^2 V}$, where V represent the tube segment volume, and V_0 its value at equilibrium. To account for finite extensibility, this is now modified to

$$p \propto c^2 \frac{a_0^2 V_0}{a^2 V} = c^2 \frac{a_0^3}{a^3} \tag{8}$$

Eq. (8) represents a FENE interchain pressure term. The scalar evolution equation for the tube diameter of Marrucci and Ianniruberto (2004) is then changed to

$$\frac{\partial a}{\partial t} = -\dot{\varepsilon} a + \frac{a_0}{\tau_a}\left(c^2 \frac{a_0^3}{a^3} - 1\right) \tag{9}$$

where τ_a has been called the tube diameter relaxation time, representing the relaxation of the topological constraints caused by the many surrounding chains (Wagner *et al.*, 2005). Considering that from Eq. (5), $\frac{\partial a}{\partial t}$ can be expressed as $\frac{\partial a}{\partial t} = -a_0 \frac{1}{\lambda^2}\frac{\partial \lambda}{\partial t}$, and replacing the first term on the right hand side of Eq. (9) by the general tensorial description using the velocity gradient tensor $\underline{\underline{\kappa}}$, the evolution equation for the stretch of a tube segment can be expressed as

$$\frac{\partial \lambda}{\partial t} = \lambda\left[(\underline{\underline{\kappa}} : \underline{\underline{S}}) - \frac{1}{\tau_a}\lambda(c^2\lambda^3 - 1)\right] = \lambda\left[(\underline{\underline{\kappa}} : \underline{\underline{S}}) - \frac{1}{\tau_a}\lambda(\lambda f^2 - 1)\right] \tag{10}$$

In Eq. (10), the first term on the right hand sides describes an affine deformation, and the second term represents the FENE interchain pressure contribution. Eq. (10) reduces to the result of Wagner *et al.* (2005) in the Gaussian limit, i.e when $c=1$ and $f=\lambda$. Eqs. (1) and (10) represent the MSF model with finite chain extensibility, and were solved numerically.

5. Refractive index tensor

For small chain extensions, the refractive index tensor is proportional to the second-moment tensor of the orientation distribution of the end-to-end vector (Fuller, 1995). According to the MSF model, the stretch is isotropic. Therefore the anisotropic part of the refractive index tensor can be obtained immediately as

$$\underline{\underline{\Delta n}}(t) = C \int_{-\infty}^{t} m(t-t')\lambda^2 \underline{\underline{S}}_{DE}^{IA}(t,t')dt' \tag{11}$$

For polystyrene, a value of the SOC of $C=-4.6\times10^{-9}\ Pa^{-1}$ is used in the following, in accordance with Luap *et al.* (2005), and supported by others (Wales, 1976; Oda *et al.*, 1978). The SOC of polystyrene is negative due to the fact that the polarizability of the polystyrene chain is smaller in the backbone direction than in a direction perpendicular to the backbone (Janeschitz-Kriegl, 1983).

6. Results and discussion

Figs. 4 and 5 present comparison of the experimental data of Luap *et al.* (2005) to predictions of the MSF theory, Eqs. (1) and (10), in the Gaussian limit, i.e. by assuming $c=1$ in Eq. (7). Both the transient elongational viscosity as well as the plateau of the elongational viscosity are well predicted for both polystyrene melts at all temperatures measured, thus supporting the results of Wagner *et al.* (2005). Slight deviations between predictions and experiments can be observed, but the differences are well within experimental error.

The optimum values of the tube diameter relaxation times τ_a were found to be 14*s* for PS206k and 71*s* for PS465k at the reference temperature of 150°C. The same WLF temperature shift factors as for the relaxation times were used. As is the case for the two highest molar mass

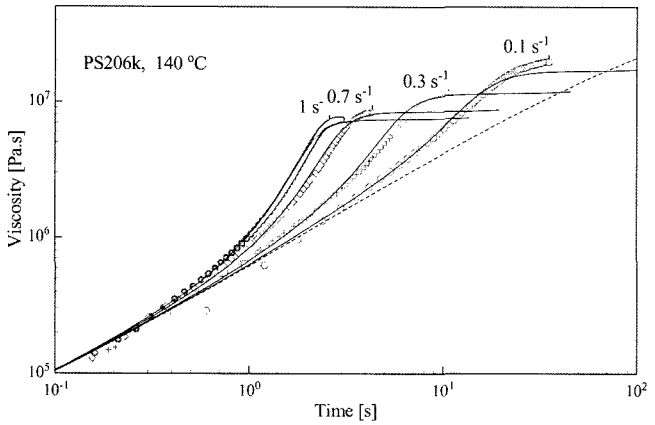

Fig. 4. Comparison of measured transient elongational viscosity data of PS206k at 140°C (symbols) to predictions by MSF model with Gaussian chain statistics (lines). Lower dotted line corresponds to the linear-viscoelastic start-up viscosity.

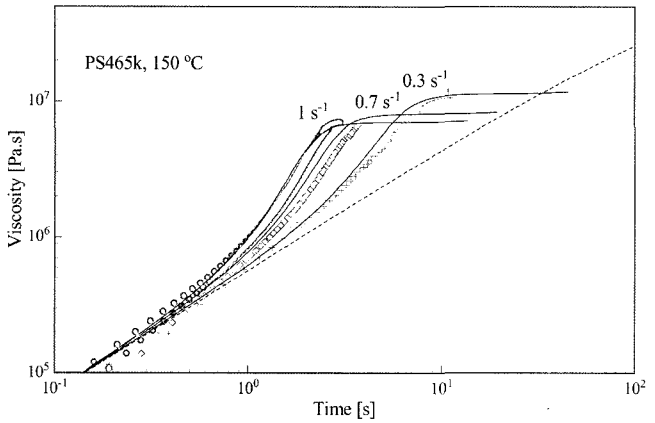

Fig. 5. Comparison of measured transient elongational viscosity data of PS465k at 150°C (symbols) to predictions by MSF model with Gaussian chain statistics (lines). Lower dotted line corresponds to the linear-viscoelastic start-up viscosity.

samples analyzed by Wagner *et al.* (2005), τ_a for PS206k and PS465k verify a quadratic dependence on the molar mass, i.e. $\tau_a \propto M^2$.

Wagner *et al.* (2005) found tube diameter relaxation times τ_a for their PS200K and PS390K as $\tau_a = 384s$ and $1462s$ respectively, at 130°C. From these values, using the WLF parameters as given by Bach *et al.* (2003) and taking into account the corrections due to the differences in molar mass by scaling with M^2, values of 9s and 47s are obtained for PS206k and PS465k respectively, at the reference temperature of 150°C. While this is not in quantitative agreement with the optimal values found here, it is at least of the same order of magnitude. The origin of the differences could be inaccuracies in the time-temperature shifting parameters or differences in the polydispersity of the samples, which might affect the amount of strain hardening observed.

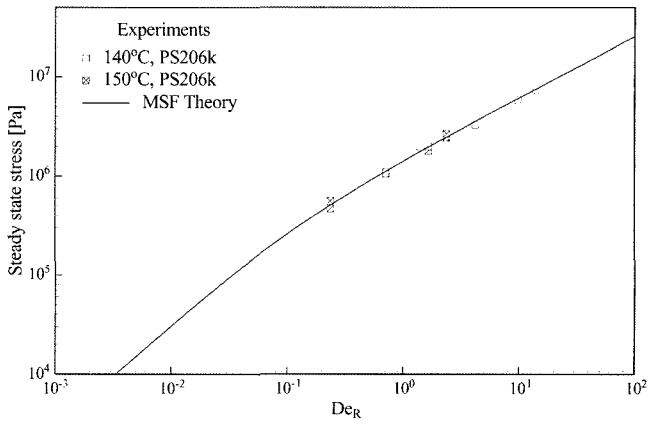

Fig. 6. Comparison of steady-state elongational stress versus Rouse-time based Deborah number $De = \varepsilon\tau_R$ to MSF predictions for PS206k at 150°C.

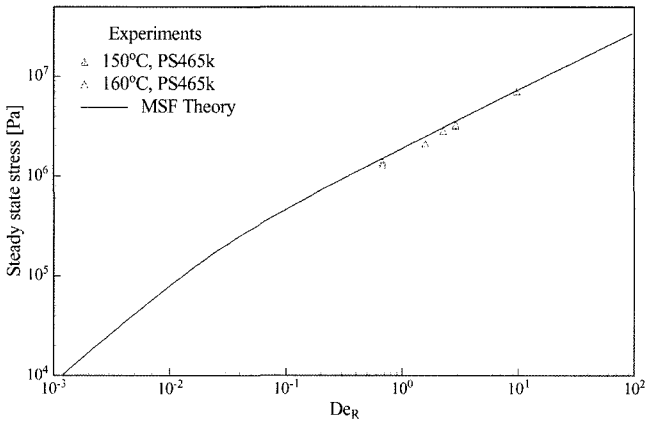

Fig. 7. Comparison of steady-state elongational stress versus Rouse-time based Deborah number $De = \varepsilon\tau_R$ to MSF predictions for PS465k (full line) at 150°C.

In Figs. 6 and 7, the steady-state stress versus a Rouse-time based Deborah number $De = \varepsilon\tau_R$ is presented, thereby using values of the Rouse times as reported by Luap *et al.* (2005) ($\tau_R = 2.4s$ for PS206k, and $\tau_R = 9.6s$ for PS465k). The agreement between predictions and experimental results is remarkable. Considering the small Deborah number limit (i.e. the Newtonian region), the difference in the zero-shear viscosities due to the different molar masses of the samples is observed. In the limit of high Deborah numbers, the two predictions tend to merge into a single curve, which indicates the transition to the glassy region and therefore to a molar mass independent response.

In the experimentally investigated central region, i.e. for $0.2 \leq De \leq 20$, different scalings for the two samples are observed: In the case of PS465k, the prediction results in a scaling relation between the steady-state stress σ_{SS} and De of the form $\sigma_{SS} \propto De^{0.59}$ in agreement with the exper-

imentally observed relation $\sigma_{SS} \propto De^{0.6\pm0.1}$ (Luap *et al.*, 2005). This coincides with the results of Wagner *et al.* (2005) for a polystyrene melt with similar molar mass (PS390K), $\eta_{SS} \propto De^{0.4}$ corresponding to $\sigma_{SS} \propto De^{0.6}$. For the PS206k sample however, a scaling relation of $\sigma_{SS} \approx De^{0.65}$ is found, indicating that the scaling relation depends on the molar mass of the melt considered. For smaller molar masses, due to the narrower plateau region of the relaxation modulus, a steeper transition from the Newtonian to the glassy region is expected. It should be emphasized that the difference in the scaling relation as predicted by the MSF model is in full agreement with the experimental data, i.e. a molar mass independent scaling relation does not exist.

While so far the discussion has been restricted to Gaussian chain statistics, the effect of finite chain extensibility (FENE) as described by the relative Padé function $c(\lambda)$ of Eq. (7) is now considered. The maximum stretch λ_m can be calculated from (van Meerveld, 2004)

$$\lambda_m = 0.82\sqrt{\frac{M_e/M_b}{C_\infty}} \tag{12}$$

The factor 0.82 takes into account the arrangement of monomer units in the 'zig-zag' conformation of the chain. M_e is the molar mass per entanglement, M_b the molar mass of the monomer and C_∞ the characteristic ratio. For polystyrene with $M_e = 18{,}100$ g·mol^{-1} (Fetters *et al.*, 1999), $M_b = 52$ g·mol^{-1} and $C_\infty = 9.46$ (Graessley, 2004), a value of $\lambda_m = 4.93$ is obtained, which is used the following.

Predictions obtained by using $c(\lambda)$ according to Eq. (7) with $\lambda_m = 4.93$ are shown in Figs. 8 and 9. It is seen that in the transient state, any observable differences between Gaussian (Figs. 4 and 5) and FENE assumptions are very small and well within the experimental accuracy for the deformation rate regime investigated. Furthermore, the steady-state elongational viscosity is invariant with respect to the approach used (Gaussian or FENE) within line width.

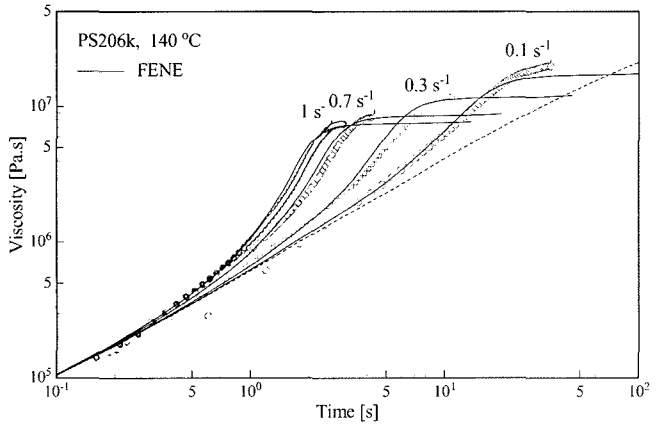

Fig. 8. Comparison of measured transient elongational viscosity data of PS206k at 140°C (symbols) to predictions by MSF model with FENE (lines) using a maximum stretch of $\lambda_m = 4.93$. Lower dotted line corresponds to the linear-viscoelastic start-up viscosity.

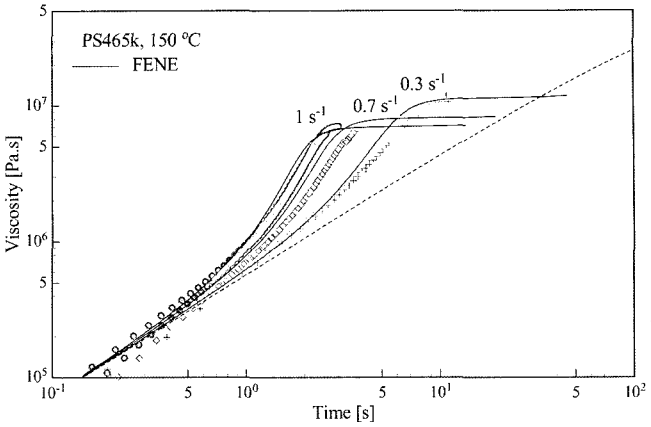

Fig. 9. Comparison of measured transient elongational viscosity data of PS465k at 150°C (symbols) to predictions by MSF model with FENE (lines) using a maximum stretch of $\lambda_m = 4.93$. Lower dotted line corresponds to the linear-viscoelastic start-up viscosity.

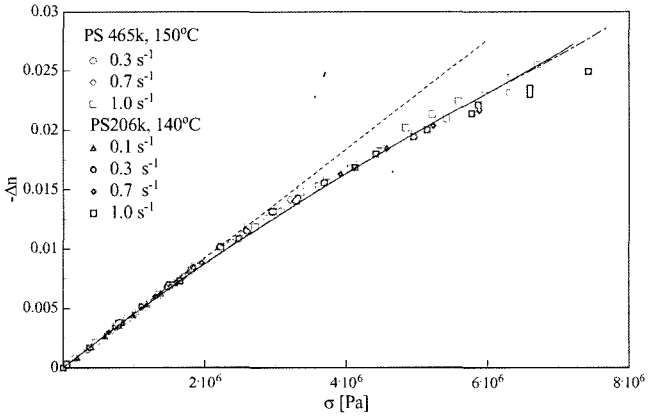

Fig. 10. Comparison of measured birefringence data versus elongational stress for PS465k at 150°C (open symbols) and PS206k at 140°C (full symbols) to MSF predictions in the Gaussian limit (dotted straight line) and with finite extensibility ($\lambda_m = 4.93$, full lines for PS465k and dash-dotted lines for PS206k).

Fig. 10 presents comparison of predictions to the measured transient values of the birefringence as a function of the transient elongational stress for both PS206k at 140°C and PS465k at 150°C. Experimental data as well as predictions superimpose for the strain rates studied, and deviate from the linear SOR (indicated by the straight dotted line in Fig. 10) noticeably above a stress of $\sigma \cong 2 \cdot 10^6$ *Pa*. Predictions and experiments agree well within experimental accuracy. The strain-rate independence of the (non-linear) SOR was already observed by others (Muller and

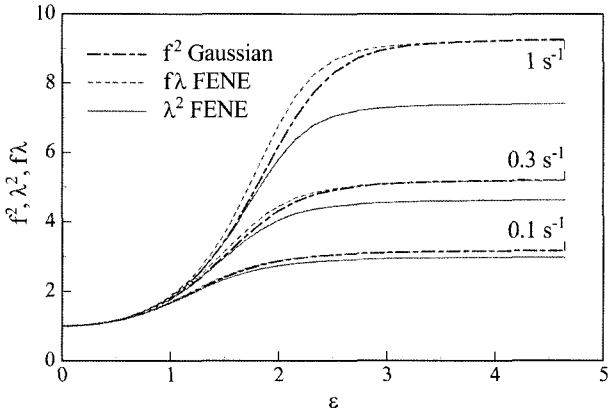

Fig. 11. Comparison of square of relative tension (identical to stretch), f^2, in the Gaussian case to square of stretch, λ^2, and product of tension and stretch, $f\lambda$, in the case of FENE using a maximum stretch of λ_m=4.93 as a function of relative Hencky strain ε for PS206k at 140°C and different strain rates.

Froelich, 1985; Muller and Pesce, 1994), and indicates that the violation of the SOR is caused by the level of chain stretch achieved, independent of strain rate. It is also obvious that the non-linear stress-optical relation is invariant with respect to temperature as well as molar mass for the monodisperse PS melts studied.

It should be noted that while the effect of finite chain extensibility on the elongational viscosity in the deformation rate range investigated is minimal, birefringence is significantly affected by non-Gaussian chain stretch, which leads to a non-linear stress-optical relation. As seen from Eq. (10), the amount of chain stretch achieved during deformation is limited essentially by the mechanical tension created. In Fig. 11, for strain rates of 0.1, 0.3, and 1.0 s^{-1}, stretch and tension are shown as a function of relative Hencky strain. In the FENE case, while for small stretches, λ^2 (determining birefringence) and the product $f\lambda$ (determining mechanical stress) nearly coincide, an increasing difference is seen at higher stretches. In the Gaussian case, i.e. assuming c=1 in Eq. (7), tension and stretch are equal, and f^2 (Gaussian case) agrees quantitatively with the FENE value of $f\lambda$ in the steady-state region, but shows small differences in the transient regime. This explains the rather small differences seen in the transient elongational viscosities between Gaussian and FENE predictions.

7. Conclusions

Elongational viscosity and birefringence data of two nearly monodisperse polystyrene melts (Luap *et al.*, 2005) were analyzed in the framework of the Molecular Stress Function (MSF) model of Wagner *et al.* (2005), which is based on the assumption of a strain-dependent tube diameter and the interchain pressure term of Marrucci and Ianniruberto (2004). The only non-linear model parameter is the tube diameter relaxation time τ_a. To model the deviations observed in the SOR, the interchain pressure term was modified to account for FENE effects using the Padé approximation of the inverse Langevin function together with a maximum stretch of λ_m=4.93. Quantitative agreement between experimental data and predictions were obtained. It was found that the tube diameter relaxation time τ_a scales with the square of the molar mass in agreement with earlier findings (Wagner *et al.*, 2005). In the strain thinning region, the steady-state elongational stress σ_{SS} scales with the Rouse-time based Deborah number De as $\sigma_{SS} \approx De^{\alpha}$. For PS465k, an exponent α=0.59 was found from the model confirming a similar result for a similar monodisperse polystyrene sample (Wagner *et al.*, 2005). For PS206k however, a higher value of α=0.65 was found from the model, showing that this scaling law is molar mass dependent with α increasing with decreasing molar mass. The value of the exponent depends on the broadness of the rubber-elastic plateau of the relaxation modulus.

The implementation of non-Gaussian chain extension has only a small effect on the predicted transient elongational viscosities in the experimental window investigated, and has no effect on the steady-state viscosities. This is due to a self-regulating limitation of chain stretch by the FENE interchain pressure term, which represents a new concept of FENE never discussed before, and which produces effectively the same value of the product of tension and stretch of the chain in the FENE case as in the Gaussian case, and therefore effectively the same value of the stress. However, finite extensibility effects are clearly seen in the birefringence data. Predictions of the MSF model with implementation of the FENE interchain pressure term and with a maximum extensibility factor of λ_m=4.93 as obtained from molecular considerations, are in excellent agreement with experimental data. In agreement with experimental evidence, the non-linear stress-optical relation is found to be invariant with respect to strain rate and temperature as well as molar mass for the two nearly monodisperse polystyrene melts in the experimental range investigated.

References

Bach, A., K. Almdal, H.K. Rasmussen and O. Hassager, 2003, Elongational viscosity of narrow molar mass distribution polystyrene, *Macromolecules* **36**, 5174-5179.

Bird, R.B., Ch.F. Curtiss, R.C. Armstrong and O. Hassager, 1987, Dynamics of Polymeric Liquids Vol. 2. Kinetic Theory, Wiley and Sons, USA.

Cathey, Ch.A. and G.G. Fuller, 1990, The optical and mechanical response of flexible polymer solutions to extensional flow, *J. Non-Newtonian Fluid Mech.* **34**, 63-68.

Cohen, A., 1991, A Padé approximant to the inverse Langevin function, *Rheol. Acta* **30**, 270-273.

Doi, M. and S.F. Edwards, 1978, Dynamics of concentrated polymer systems. Part 2.- Molecular motion under flow, *J. Chem. Soc., Faraday Trans. 2* **74**, 1802-1817.

Doi, M. and S.F. Edwards, 1979, Dynamics of concentrated polymer systems. Part 4.- Rheological properties, *J. Chem. Soc., Faraday Trans. 2* **75**, 38-54.

Fan, B., D.O. Kazmer, W.C. Bushko, R.P. Theriault and A.J. Poslinski, 2004, Biregringence prediction of optical media, *Polym. Eng. Sci.* **44**, 814-824.

Fang, G., M. Kröger and H.C. Öttinger, 2000, A thermodynamically admissible reptation model for fast flows of entangled polymers. II. Model predictions for shear and extensional flows, *J. Rheol.* **44**, 1293-1317.

Fetters, L.J., D.J. Lohse, S.T. Milner and W.W. Graessley, 1999, Packing length influence in linear polymer melts on the entanglement, critical, and reptation molecular weights, *Macromolecules* **32**, 6847-6851.

Fuller, G.G., 1995, Optical Rheometry of Complex Fluids, Oxford University Press, New York.

Graessley, W.W., 2004, Polymeric Liquids and Networks: Structure and Properties, Garland Science, New York.

Hua, Ch.C. and J.D. Schieber, 1998, Segment connectivity, chain-length breathing, segmental stretch, and constraint release in reptation models. I. Theory and single-step strain predictions, *J. Chem. Phys.* **109**, 10018-10027.

Inoue, T, H. Okamoto and K. Osaki, 1991, Birefringence of amorphous polymers. 1. Dynamic measurements on polystyrene, *Macromolecules* **24**, 5670-5675.

Janeschitz-Kriegl, H., 1983, Polymer Melt Rheology and Flow Birefringence, Springer-Verlag, Berlin.

Kotaka, T., A. Kojima and M. Okamoto, 1997, Elongational flow opto-rheometry for polymer melts- 1. Construction of an elongational flow opto-rheometer and some preliminary results, *Rheol. Acta* **36**, 646-656.

Kröger, M., C. Luap and R. Muller, 1997, Polymer melts under uniaxial elongational flow: Stress-optical behavior from experiments and nonequilibrium molecular dynamics computer simulations, *Macromolecules* **30**, 526-539.

Larson, R.G., 1988, Constitutive Equations for Polymer Melts, Butterworths, Stoneham.

Lodge, A.S., 1955, Variation of Flow Birefringence with Stress, *Nature* **176**, 838-839.

Luap, C., Ch. Müller, T. Schweizer, and D.C. Venerus, 2005, Simultaneous stress and birefringence measurements during uniaxial elongation of polystyrene melts with narrow molecular weight distribution, *Rheol. Acta* **45**, 83-91.

Marrucci, G. and N. Grizzuti, 1988, Fast flows of concentrated polymers: Predictions of the tube model on chain stretching, *Gazz Chim Italiana* **118**, 179-185.

Marrucci, G. and G. Ianniruberto, 2004, Interchain pressure effect in extensional flows of entangled polymer melts, *Macromolecules* **37**, 3934-3942.

Matsumoto, T. and D.C. Bogue, 1977, Stress birefringence in amorphous polymers under nonisothermal conditions, *J. Polym Sci. Polym. Phys.* **15**, 1663-1674.

Mead, D.W. and R.G. Larson, 1990, Rheoptical study of isotropic solutions of stiff polymers, *Macromolecules* **23**, 2524-2533.

Mead, D.W. and L.G. Leal, 1995, The reptation model with segmental stretch. I. Basic equations and general properties, *Rheol. Acta* **34**, 339-359.

Mead D.W., R.G. Larson and M. Doi, 1998, A molecular theory for fast flows of entangled polymers, *Macromolecules* **31**, 7895-7914.

Muller, R. and D. Froelich, 1985, New extensional rheometer for elongational viscosity and flow birefringence measurements: some results on polystyrene melts, *Polymer* **26**, 1477-1482.

Muller, R. and J.J. Pesce, 1994, Stress-optical behaviour near the Tg and melt flow-induced anisotropy in amorphous polymers, *Polymer* **35**, 734-739.

Oda, K., J.L. White and E.S. Clark, 1978, Influence of melt deformation history on orientation in vitrified polymers, *Polym. Eng. Sci.* **18**, 53-59.

Öttinger, H.C., 1999, A thermodynamically admissible reptation model for fast flows of entangled polymers, *J. Rheol.* **43**, 1461-1493.

Pearson, D.S., E. Herbolzheimer, N. Grizzuti and G. Marrucci, 1991, Transient behavior of entangled polymers at high shear rates, *J. Polym. Sci. B: Polym. Phys.* **29**, 1589-1597.

Pellens, L., J. Vermant and J. Mewis, 2005, Deviations from the stress-optical rule in telechelic associative polymer solutions, *Macromolecules* **38**, 1911-1918.

Philippoff, W., 1956, Flow-birefringence and stress, *Nature* **178**, 811-812.

Rothstein, J.P. and G.H. McKinley, 2002, A comparison of the stress and birefringence growth of dilute, semi-dilute and concentrated polymer solutions in uniaxial extensional flows, *J. Non-Newtonian Fluid Mech.* **108**, 275-290.

Sridhar, T., D.A. Nguyen and G.G. Fuller, 2000, Birefringence and stress growth in uniaxial extension of polymer solutions, *J. Non-Newtonian Fluid Mech.* **90**, 299-315.

Subramanian, P.R. and V. Galiatsatos, 1993, Stress-optical properties of bimodal polymer networks, *Makromol. Chem., Macromol. Symp.* **76**, 233-240.

Talbott, W.H. and J.D. Goddard, 1979, Streaming birefringence in extensional flow of polymer solutions, *Rheol. Acta* **18**, 505-517.

van Meerveld, J., 2004, Validity of the linear stress optical rule in mono-, bi- and polydisperse systems of entangled linear chains, *J. Non-Newtonian Fluid Mech.* **123**, 259-267.

Venerus, D.C., S.-H. Zhu and H.C. Öttinger, 1999, Stress and birefringence measurements during the uniaxial elongation of polystyrene melts, *J. Rheol.* **43**, 795-813.

Wagner, M.H., 1990, The nonlinear strain measure of polyisobutylene melt in general biaxial flow and its comparison to the Doi-Edwards model, *Rheol. Acta* **29**, 594-603.

Wagner, M.H. and J. Schaeffer, 1992, Nonlinear measures for general biaxial extension of polymer melts, *J. Rheol.* **36**, 1-26.

Wagner, M.H., P. Rubio and H. Bastian, 2001, The molecular stress function model for polydisperse polymer melts with dissipative convective constraint release, *J. Rheol.* **45**, 1387-1412.

Wagner, M.H., M. Yamaguchi and M. Takahashi, 2003, Quantitative assessment of strain hardening of low-density polyethylene melts by the molecular stress function model, *J. Rheol.*

47, 779-793.

Wagner, M.H., S. Kheirandish and O. Hassager, 2005, Quantitative prediction of transient and steady-state elongational viscosity of nearly monodisperse polystyrene melts, *J. Rheol.* **49**, 1317-1327.

Wales, J.L.S., 1976, The Application of Flow Birefringence to Rheological Studies of Polymer Melts, Delft University Press.

Winter, H.H. and M. Mours, 2003, IRIS Developments, http://rheology.tripod.com/.

Ye, X. and T. Sridhar, 2005, Effects of the polydispersity on rheological properties of entangled polystyrene solutions, *Macromolecules* **38**, 3442-3449.